NASA Contractor Report 177601

Effect of Non-Equilibrium Flow Chemistry on the Heating Distribution Over the MESUR Forebody During a Martian Entry

Yih-Kang Chen

CONTRACT NAS2-13210
September 1992

National Aeronautics and
Space Administration

NASA Contractor Report 177601

Effect of Non-Equilibrium Flow Chemistry on the Heating Distribution Over the MESUR Forebody During a Martian Entry

Yih-Kang Chen

Sterling Federal Systems, Inc.
1121 San Antonio Road
Palo Alto, CA 94303-4380

Prepared for
Ames Research Center
CONTRACT NAS2-13210
September 1992

National Aeronautics and
Space Administration

Ames Research Center
Moffett Field, California 94035-1000

Table of Contents

Nomenclature

C_i	mass fraction of species i
J_i	diffusion flux of species i
k_i	surface catalytic recombination
k_f	forward reaction rate coefficient
k_b	backward reaction rate coefficient
M_i	molecular weight
q_s	stagnation point heat flux
R	gas constant
Rb	base radius
R_{eff}	effect nose radius
R_n	nose radius
T	temperature
T_w	wall temperature
V_e	entry velocity
Z	third body reaction rate
α_{ri}	stoichiometric coefficient for reactants
β_{ri}	stoichiometric coefficient for products
δ	cone half angle
ρ_i	density
γ_i	recombination coefficient
ω_i	mass production rate

0.0 Summary

Effect of flow field properties on the heating distribution over a 140° blunt cone was determined for a Martian atmosphere using Euler, Navier-stokes (NS), viscous shock layer (VSL) and reacting boundary layer (BLIMPK) equations. Effect of gas kinetics on the flow field and surface heating distribution were investigated. Gas models with nine species and nine reactions were implemented into the codes. Effects of surface catalysis on the heating distribution were studied using a surface kinetics model having five reactions.

1.0 Introduction

Analysis of hypersonic CO_2 flows plays an important role in the design of thermal protection system (TPS) for the Mars Environmental Survey Vehicle (MESUR). The proposed configuration for MESUR is a large-angle blunt cone with a cone-half-angle of 70°, base radius of 0.85 m and a bluntness ratio of Rn/Rb = 0.5, Fig.1. Evens et al used an inverse method with infinite rate chemistry to study the effect of ablation in a shock layer with non-equilibrium inviscid flow on the Viking radio blackout.[1] Recently, Candler solved two-dimensional axisymmetric Navier-Stokes equations with multiple species and temperatures to simulate the flow environment in front of a large-angle cone during its high-speed aerobraking maneuvers through the Martian atmosphere.[2]

The gas kinetics model used in both studies came mostly from the work of McKenzie.[3] Since then, an extensive study on gas kinetics modeling for the Martian atmosphere has been made by Park et al.[4] In this study, both gas kinetics models are used in Viscous Shock Layer (VSL)[5,12] and Navier-Stokes (NS)[2,6] codes to simulate the flow between the bow shock wave of the MESUR vehicle during its entry into the Martian atmosphere. The NS code was modified to include Park's kinetics and third body reactions with different reaction rates. The flow near the surface of the vehicle's heat shield, was simulated using the Boundary Layer Integral Matrix Procedure with kinetics (BLIMPK).[7] The thermodynamic properties used in all the codes were obtained from the Janaf Tables.[8]

The purpose of this study is to estimate the effect of gas and surface kinetics on the heat flux to TPS of the MESUR vehicle, during a Martian entry.

Inviscid Flow Field

Inviscid flow properties at the surface of the heat shield were calculated using the Ames Method of Integral Relations (AMIR)[9] which is based on the methodology developed by Belotserkovskiy.[10] The region between the body and bow shock wave is divided into strips and the variations of the flow properties across the shock layer are represented by polynomials which depend upon the number of strips. Conditions of regularity proposed by Belotserkovskiy are not included in AMIR, therefore the system of equations are not closed and no unique solution exists. However an optimized solution, which is based on the location of the sonic point on the body, can be obtained. The structure of AMIR has been reorganized for running on the modern super compute and these solutions agree well with the old version of AMIR.

Inviscid flow properties calculated using AMIR included pressure and velocity. The pressure distribution over the surface of the MESUR heat shield calculated using the one-strip (solid line) and two-strip (dashed line) methods are shown in Fig.2. In general, the two-strip method predicts a higher surface pressure over the forebody of the vehicle and higher pressure gradients at the corner of the vehicle than the one-strip method. The pressure distribution calculated from AMIR is used in BLIMPK to calculate the heating distribution over the MESUR forebody heat shield.

Reacting Viscous Flow

Reacting flow properties in the shock layer were calculated using BLIMPK, NS and VSL codes. These codes were developed to simulate non-equilibrium air flows over spacecraft TPS during their high speed aerobraking maneuvers. The reacting boundary layer, next to the body, was simulated using BLIMPK as outlined in Ref. 12. BLIMPK is a laminar non-similar multi-component boundary layer procedure, which contains gas phase kinetics and rate controlled surface reactions. The governing equations are discretized in integral matrix form and solved by Newton-Raphson iteration.

The NS and VSL codes were used to simulate the flow throughout the shock layer. In the NS code, fluid dynamics of a multiple-species two temperature gas kinetics model was characterized by a set of partial differential equations. They are essentially the two-dimensional axisymmetric NS equations expanded to account for the presence of multiple species and temperatures. The equations are solved in a fully coupled manner; using implicit, flux split, Gauss-Seidel line relaxation numerical techniques.[3]

The VSL governing equations are a subset of the NS equations and are obtained by retaining up to second order terms in the inverse square-root of the Reynolds number. VSL analysis is valid through the shock layer to moderately low Reynolds number and provides a direct means of accounting for the interactions between the inviscid and viscous flow regimes behind the bow shock wave. The governing equations are solved by a finite-difference method and using an initial global solution obtained assuming a thin viscous shock layer. Subsequent global iterations are made assuming a fully viscous shock layer between the body and bow shock wave.

Chemical Kinetics Model

Nine species (O, O2, N, N2, NO, C, CO, CO2 and Ar) gas model with nine reactions imployed in the reacting viscous flow codes are given below:

$$O2 + M1 = 2O + M1$$

$$N2 + M2 = 2N + M2$$

$$NO + M3 = N + O + M3$$

$$NO + O = O2 + N$$

$$N2 + O = NO + N$$

$$CO2 + M4 = CO + O\ M4$$

$$CO + M5 = O + O\ M5$$

$$CO2 + O = O2 + CO$$

$$CO + O = O2 + O$$

where M represents any specie that acts as a collisional partner. Each reaction is governed by a forward and backward reaction rate coefficient, kf and kb, respectively (Tables 1 and 2).

If the rate of production terms in the continuity and energy equations are rewritten so that the specie concentration and temperature appear as the unknowns [13], then the terms used in the VSL code result in the following expressions,

$$\frac{\omega_i}{\rho} = \omega^0{}_i - \omega^1{}_i\, C_i \ ;$$

$$\frac{\partial}{T}\left(\frac{\omega_i}{\rho}\right) = \frac{M_i}{T}\sum_{r=1}^{nr}(\beta_{ri} - \alpha_{ri})\left[\left(C2_r + \frac{C1_r}{T} - \alpha_r\right) L_{fr} - \left(D2_r + \frac{D1_r}{T} - \beta_r\right) L_{br}\right] \ ;$$

where

$$\omega^0{}_i = M_i \sum_{r=1}^{nr} (\Gamma^+{}_{ri} L_{fr} + \Gamma^-{}_{ri} L_{br}) \ ;$$

$$\omega^1{}_i = \sum_{r=1}^{nr}\left[\Gamma^+{}_{ri}\frac{L_{br}}{r_i} + \Gamma^-{}_{ri}\frac{L_{fr}}{r_i}\right] \ ;$$

$$r_i = \frac{C_i}{M_i} \ ; \qquad i=1,2,...,ns \ ;$$

$$r_i = \sum_{j=1}^{ns} Z_{(i-ns)_j} r_j \ ; \qquad i= (ns+1),\ ....,\ (ns+5) \ ;$$

$$L_{fr} = k_{fr}\rho^{\alpha r}\prod_{j=1}^{nj} r_j{}^{\alpha_{rj}} \ ;$$

$$L_{br} = k_{br}\rho^{\beta r}\prod_{j=1}^{nj} r_j{}^{\beta_{rj}}$$

$$\alpha_r = \sum_{j=1}^{nj}\alpha_{rj}\text{-}1 \ ; \quad \beta_r = \sum_{j=1}^{nj}\beta_{rj}\text{-}1 \ ;$$

$$\Gamma^+{}_{ri} = \beta_{ri} - \alpha_{ri} \quad \text{if } (\beta_{ri} - \alpha_{ri} > 0 \quad \text{else } \Gamma^+{}_{ri} = 0 \ ;$$

$$\Gamma^-{}_{ri} = -(\beta_{ri} - \alpha_{ri}) \quad \text{if } (\beta_{ri} - \alpha_{ri}) < 0 \quad \text{else } \Gamma^-{}_{ri} = 0 \ .$$

Surface Reactions

Stewart has demonstrated by flight experiments that surface catalysis can have a major effect on the surface heat flux to a thermal protection system (TPS).[11] These data were correlated with predictions of the surface heating distribution along the midfuselage of the Space Shuttle using first order surface kinetic reactions in BLIMPK. The surface reactions consider in this study are also assumed as first order reactions,

0.5N + 0.5N -> 0.5N2

0.5O + 0.5O -> 0.5O2

0.5N + 0.5O -> 0.5NO

0.5C + 0.5O -> 0.5CO

0.5CO + 0.5O -> 0.5CO2

and the reaction rates are,

$$k_i = \gamma_i (RT_w/2\pi M_i)^{(1/2)}; \qquad i=1 \text{ to } 5 \ ;$$

Reaction 1: $J^1_N = -k_1 \rho_N$, $J^1_{N2} = k_1 \rho_N$;

Reaction 2: $J^2_O = -k_2 \rho_O$, $J^2_{O2} = k_2 \rho_O$;

Reaction 3: $J^3_O = -k_3 (\rho_N \rho_O)^{(1/2)}$, $J^3_N = -k_3 \frac{M_N}{M_O} (\rho_N \rho_O)^{(1/2)}$,

$$J^3_{NO} = k_3 \frac{M_{NO}}{M_O} (\rho_N \rho_O)^{(1/2)} \ ;$$

Reaction 4: $J^4_O = -k_4 (\rho_C \rho_O)^{(1/2)}$, $J^4_C = -k_4 \frac{M_C}{M_O} (\rho_C \rho_O)^{(1/2)}$,

$$J^4_{CO} = k_4 \frac{M_{CO}}{M_O} (\rho_C \rho_O)^{(1/2)};$$

Reaction 5: $J^5_O = -k_5 (\rho_{CO} \rho_O)^{(1/2)}$, $J^5_{CO} = -k_5 \frac{M_{CO}}{M_O} (\rho_{CO} \rho_O)^{(1/2)}$,

$$J^5_{CO2} = k_5 \frac{M_{CO2}}{M_O} (\rho_{CO} \rho_O)^{(1/2)}.$$

These surface reactions, with specific reaction rates, were imployed in BLIMPK and VSL. In the NS code , the effect of surface catalysis on the heat flux to the TPS is not included and the surface was assumed to be isothermal (Tw = 1700 K) and non-catalytic. BLIMPK predicted the heat flux to the TPS with the assumption that the boundary edge properties were in thermal and chemical equilibrium.

Results and Discussion

The convective heat flux to the MESUR heat shield during its high-speed aerobraking maneuvers in the Mars atmosphere results from both sensible and chemical heating. Sensible heating to large-angle blunt cones has been shown to be dependent on cone angle and bluntness ratio. [14,15] In air, the stagnation point heat flux varies directly with the ratio of the square root of the velocity gradients calculated from AMIR and the value calculated using Newtonian theory.[14]

$$\frac{q_{st}}{q_{\delta=50}} = \left[\frac{(du/ds)_{AMIR}}{(du/ds)_{Newtonoan}}\right]^{(1/2)}$$

where:

$$(du/ds)_{Newtonian} = \frac{1}{Rn}\left(\frac{2P_{st}}{\rho_{st}}\right)^{(1/2)}$$

A similar relationship for large-angle blunt cones is shown for CO_2 in Fig. 3. The figure shows that the sensible heating to the stagnation point of the MESUR is 30% to 40% lower than to a conical shape with a half-angle of 50^0, where the velocity gradient is predicted by Newtonian theory.

The chemical heating portion of the convective heat flux is dependent upon the non-equilibrium flow properties in the shock layer and surface catalysis.

Predicted non-equilibrium flow properties along the stagnation point stream line obtained using Park's and McKenzie's gas kinetics models in VSL, NS and BLIMPK codes are compared in Fig.4 thru Fig.7. Trajectories points were chosen near where peak heating occurs, Alt. = 40.427 km and V = 5 km/sec (condition 1) and an Alt. = 41.668 and V = 7 km/sec (condition 2).

Predicted specie concentration profiles along the stagnation stream-line are compared in Fig.4. The predictions were made using Park's gas kinetics model in NS (solid lines), VSL (dash-lines) and BLIMPK (dotted-lines) solutions. The profiles from three solutions agree well in the region near the surface of the heat shield, but deviate through the shock layer.

Next, the effect of the gas kinetics models on the predicted flow properties along the stagnation stream-line are compared in Fig.5 and Fig.6. Fig.5, compares the gas temperature distribution throughout the shock layer using VSL solutions for flight condition 1. The gas temperature throughout the shock layer predicted using McKenzie's model is higher than values predicted using Park's, because more energy is released by the CO2 recombination near the shock. Also, the surface temperature is higher (200 K) than the value predicted using Park's gas kinetics model. The effect of the gas kinetics model on the specie concentration profiles are shown in Fig.6. In the high temperature regime (near the bow shock wave), Park's kinetics model predicts higher dissociation of CO2 than McKenzie's kinetics model, but in the lower temperature regime (near the surface) McKenzie's model predicts much higher recombination rates than Park's model. Specie concentration profiles obtained from NS solutions for flight condition 2 are compared in Fig.7. These profiles are consistent with the results plotted in Fig.6.

The effect of the gas kinetic models and surface catalysis on the heating distribution over the MESUR forebody heat shield is illustrated in Fig. 8. The VSL and BLIMPK solutions were performed assuming the heat shield surface to be fully catalytic as well as noncatalytic. For the case where the surface is assumed as fully catalytic, the heating distribution over the heat shield is independent of the gas kinetics models for CO_2 and O_2 used in the calculation. However, for a non-catalytic surface the model used in the solutions had a large effect on the heating distribution. For both solutions, McKenzie's model resulted in higher heating rates to the non-catalytic surface than the values calculated using Park's model. The largest difference in the heating rates occurred using the BLIMPK solution where the values were higher than those calculated for recombination of O_2 to a fully catalytic surface, Fig.8a. Using McKenzie's model in the VSL solution resulted in slightly higher heating rates over the conical portion, but lower values near the stagnation region of the non-catalytic surface than predicted for the recombination of O_2 to a fully catalytic surface,Fig.8b. This phenomenon is the result of oxygen atom starvation of the CO recombination reactions; i.e. the oxygen recombination on the surface consumes most of the oxygen atoms ($O + O \rightarrow O_2$), thus it reduces the available oxygen atoms for CO_2 recombination ($CO + O \rightarrow CO_2$). Surface heating distribution over the heat shield was not predicted using the NS code because of numerical difficulty encountered around the stagnation stream-line region and the code was not configured to the flow with coupled energy balance and surface catalysis.

The shock stand-off distance predicted by VSL was about 17% smaller than the value predicted using the NS code. The difference is the result of assuming an infinite body length in the VSL solution,and using the actual body geometry in the NS solution where the feedback effects from corner are included in the prediction of the shock stand-off distance. Therefore, it follows that the velocity gradient at the stagnation point is close to a value predicted by Newtonian theory and the heating rate to the MESUR is lower than predicted by the VSL code, see Fig. 3.

The nose radius used in the VSL solution was adjusted using Eq. 1 to reflect the difference between a velocity gradient predicted by Newtonian theory and one predicted by AMIR for the MESUR vehicle. Effect of nose radius on the heating distribution over the heat shield using VSL with Park's gas kinetics model is shown in Fig.9. In addition to the present flight case (V = 7 km/s), a solution was also performed for V = 9 km/s. Stagnation point heating rates in both cases were reduced about 30% by using the effective nose; thus the results are consistent with Fig.3.

2.0 Conclusion

This study shows the predictions of flow fields as well as surface heat transfer rates are very sensitive to both gas and surface kinetics. The accuracy of available gas kinetics should be carefully reexamined at high and low temperatures. So far, no research has been conducted to understand the surface kinetics of CO2 flows! Without the knowledge of CO2 surface catalysis, the accurate prediction of surface heating over Thermal Protection System is unlikely. In addition, no engineering tool is available for the analysis of flows over high angle blunted bodies (> 60 degrees) at low Reynolds number. BLIMPK is useful for flows with relatively high Reynolds number only, and the boundary layer nonequilibrium edge conditions have to be estimated using NS or VSL. The VSL code fails to predict the corner effect, and becomes quite unstable as the cone half-angle becomes large. Most of current available NS solvers encounter numerical difficulty around the stagnation stream line region as the cone half-angle is large. Current NS solution with coupled surface energy balance and catalysis are too expensive and time consuming for either arcjet or design of TPS.

3.0 References

1. J. S. Evans, C. J. Schexnayder Jr., and W. L. Grose, "Effects of Nonequilibrium Ablation Chemistry on Viking Radio Blackout", J. Spacecraft, Vol. 11, No. 2, pp. 84-88, 1974.

2. G. V. Candler, "Computation of Thermo-Chemical Non-equilibrium Martian Atmospheric Entry Flows", AIAA 90-1695.

3. R. L. McKenzie, "An Estimate of the Chemical Kinetics Behind Normal Shock Waves in Mixtures of Carbon Dioxide and Nitrogen for Conditions Typical of Mars Entry", NASA TN D-3287.

4. C. Park, J. T. Howe, R, L. Jaffe, and G. V. Candler, "Chemical-Kinetics Problems of future NASA Missions", AIAA 91-0464.

5. R. N. Gupta and A. L. Simmonds, "Stagnation Flowfield Analysis for Aeroassist Flight Experiment Vehicle", AIAA paper 88-2613.

6. G. V. Candler, and R. W. MacCormack, "The Computation of Hypersonic Ionized Flows in Chemical and Thermal Nonequilibrium", AIAA paper 88-0511.

7. E. P. Bartlett, and R. M. Kendall, "An Analysis of the Coupled Chemically Reacting Boundary Layer and Charring Ablator, Part III: Nonsimilar Solution of the multi-component Laminar Boundary Layer by Integral Matrix Method", NASA CR-1062.

8. "User's Manual: Aerothermal Chemical Equilibrium Computation Program", Acurex Report UM-81-11/ADT.

9. M. Inouye, "Numerical Solution by the Method of Integral Relations of the Flow Field Around Flat-Faced Bodies Traveling at supersonic Speed", Private Communication.

10. O. M. Beloserkovskiy, "Supersonic Gas Flow Around Blunt Bodies", NASA TT F-453.

11. D. A. Stewart, J. V. Rakich, and M. J. Lanfrance, "Catalytic Surface Effects on Space Shuttle Thermal Protection System During Earth Entry of Flights SDTS-2 through STS-5", NASA CP 2283.

12. D. A. Stewart, Y.-K. Chen, and W. D. Henline, "Effect of Non-equilibrium Flow Chemistry and Surface Catalysis on Surface Heating to AFE", AIAA paper 91-1373.

13. R. T. Davis, "Numerical Solution of the Hypersonic Viscous Shock-Layer Equations", AIAA J., Vol. 8, pp.834-851, 1970.

14. D. A. Stewart, and P. Kolodziej, "Heating Distribution Comparison between Asymmetric and symmetric Blunt cones", AIAA paper 86-1307.

15. D. A. Stewart and J. G. Marvin, "Convective Heat-Transfer Rates on large-angle Conical Bodies at Hypersonic Speeds", NASA TN 5526.

Fig. 1, MESUR ENTRY VEHICLE

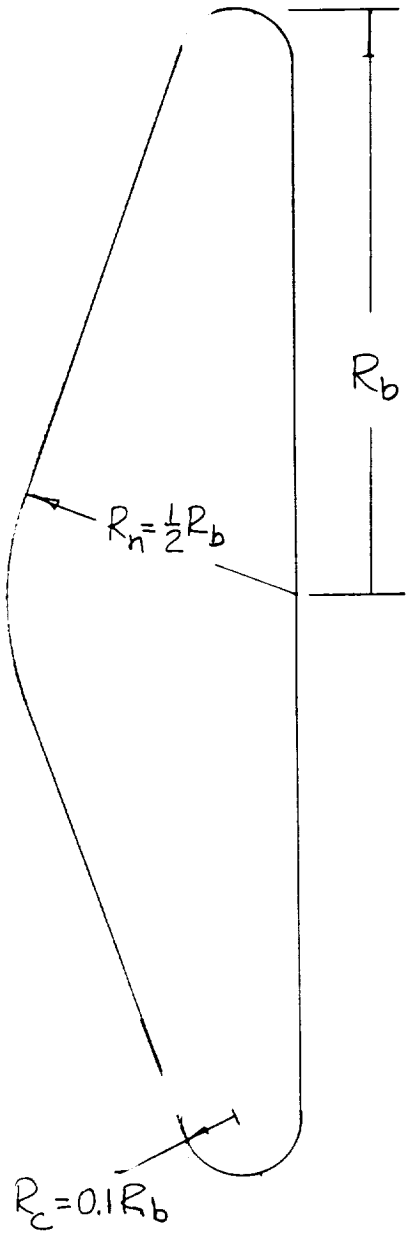

Fig. 2: Pressure Distributions over Surface
70-degree sphere cone; Rn/Rb = 0.2

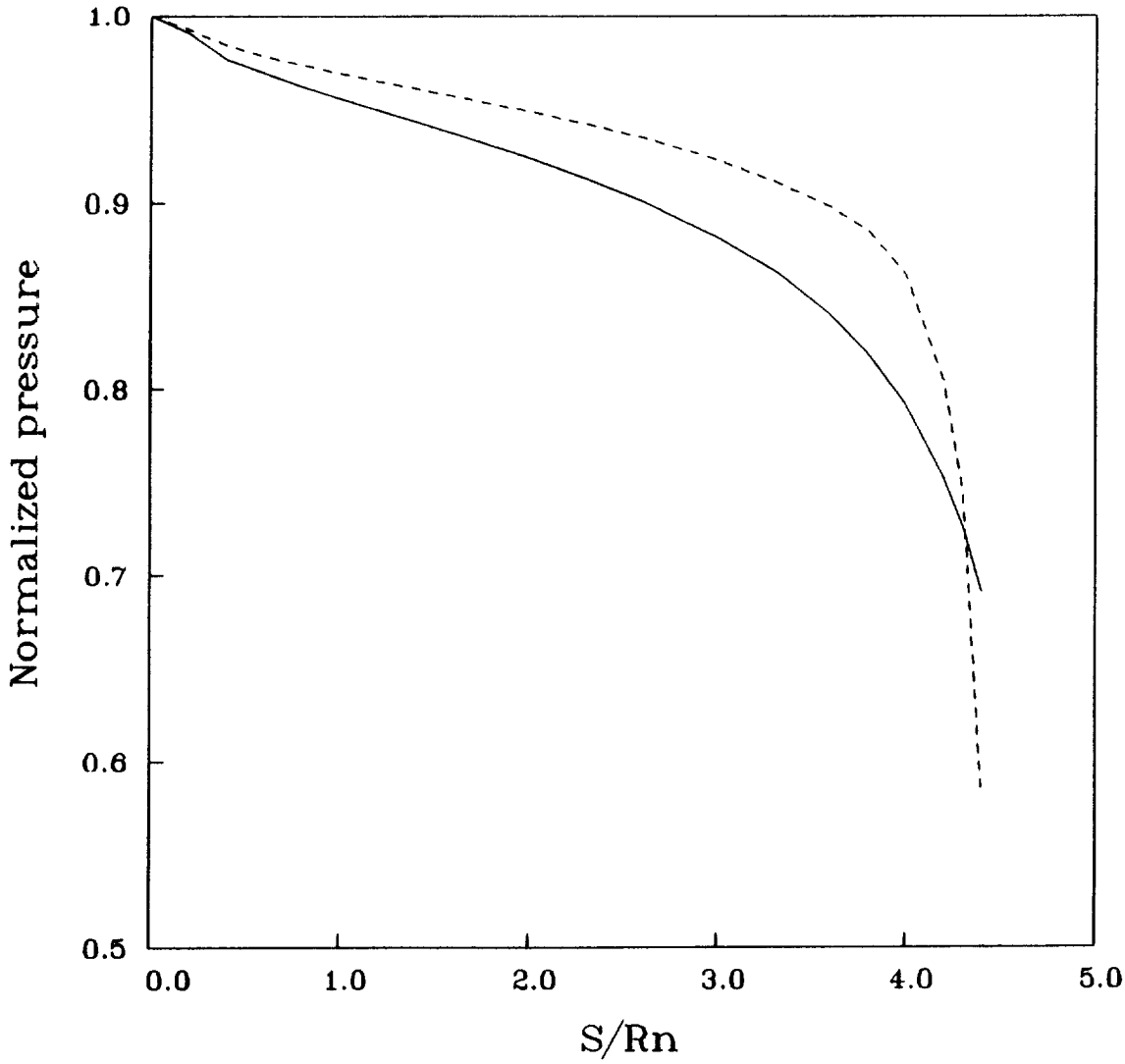

Solid line: one-strip solution
Dashed line: two-strip solution
Gamma = 1.2

Fig. 3: Effect of Cone Angle on Stagnation Point Heating

Gamma = 1.2; AMIR solutions

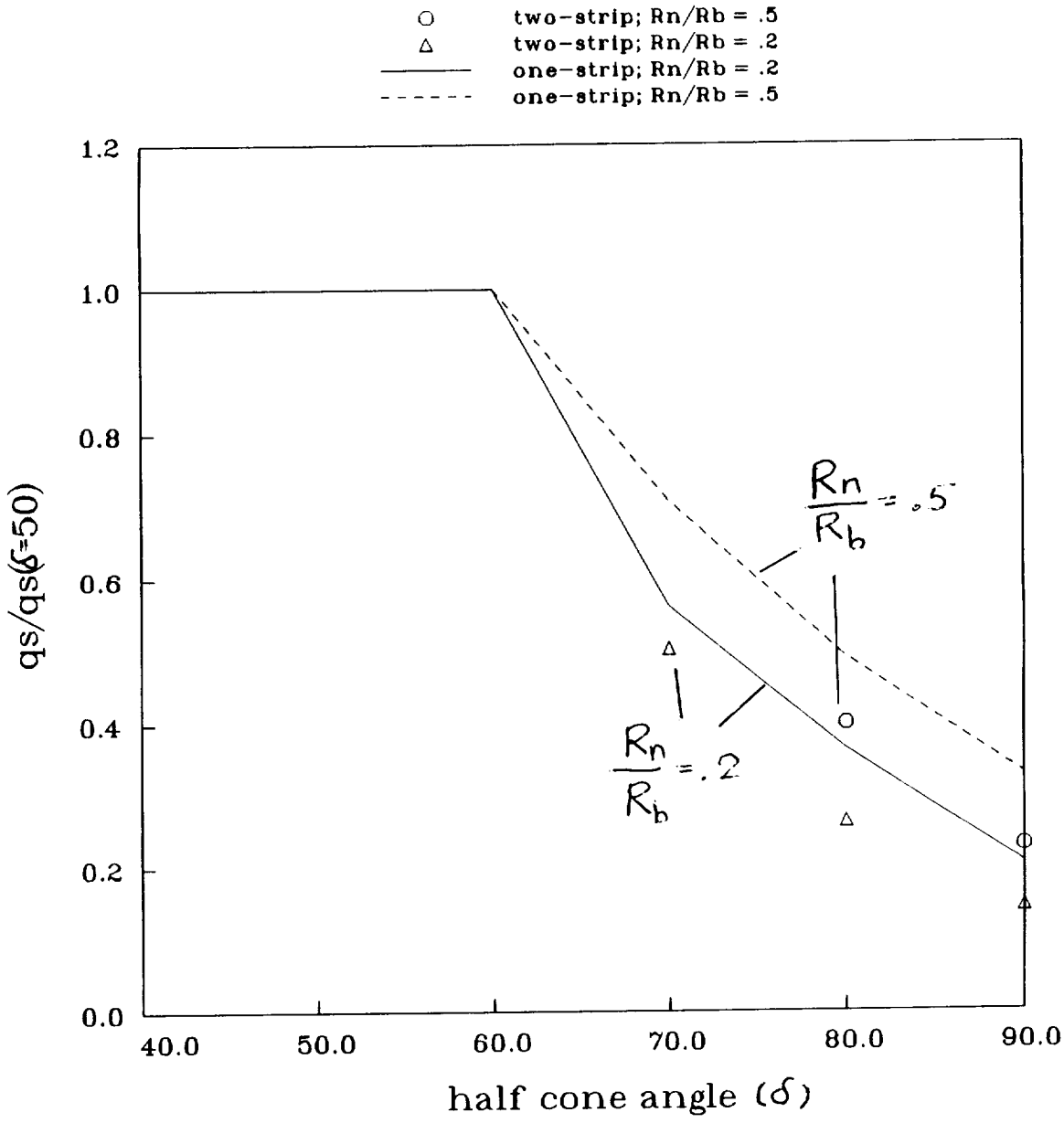

Fig.4: Mass Fractions Along Stagnation Streamline
NCW with Tw = 1700 K; Ve = 7 km/sec; Rn = 0.425 m

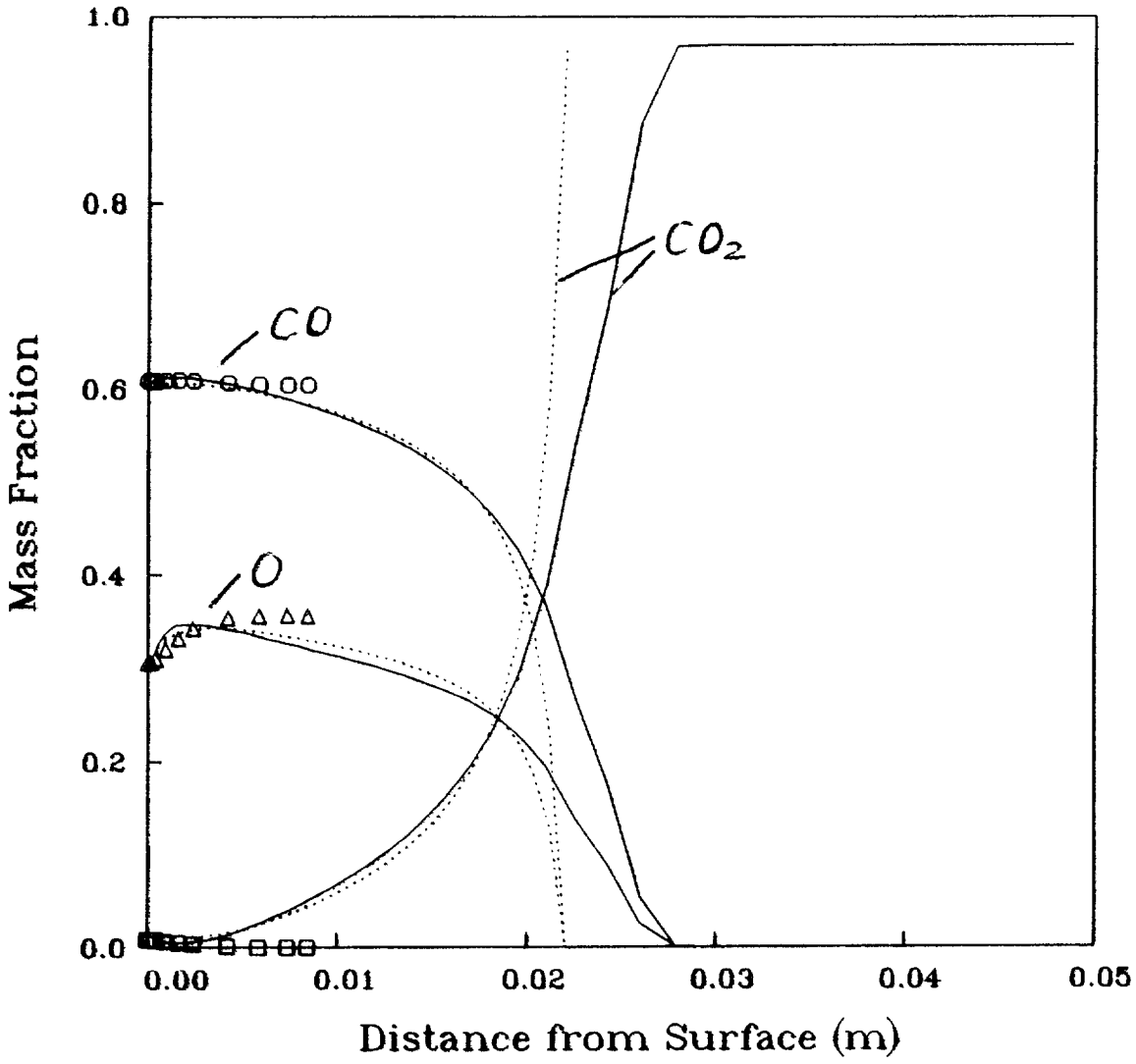

Solid lines: Navier–Stokes solution
Symbols: BLIMP with equil. edge
Dotted lines: VSL solution
Park's kinetics

Fig5: Temperature along Stagnation Streamline
70-degree sphere-cone; NCW; REQW; Ve = 5 km/sec

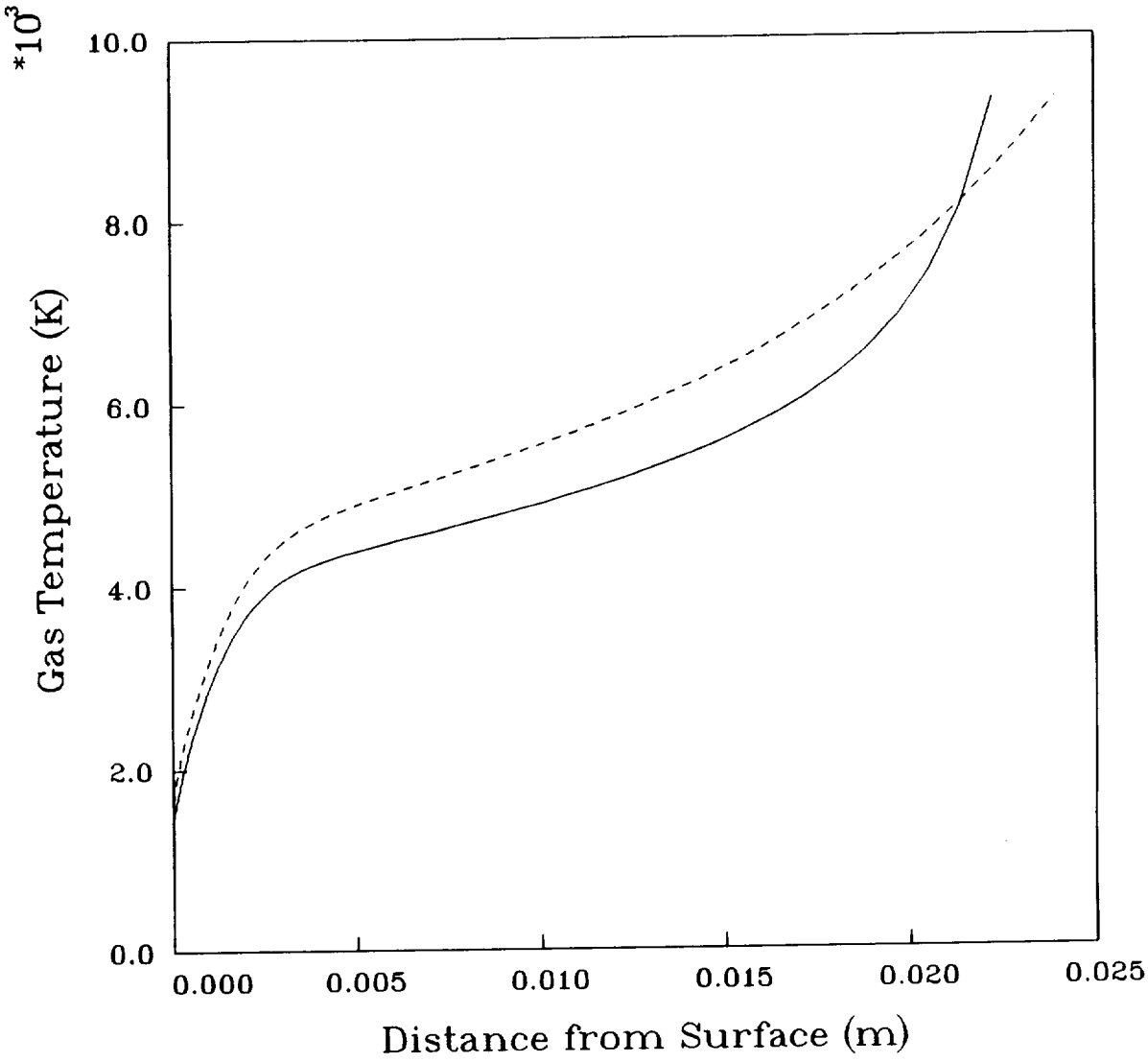

solid line: Park's kinetics
dashed line: McKenzie's kinetics
VSL solution

Fig 6: Species profiles along Stagnation Streamline
70-degree sphere-cone; NCW; REQW; Ve = 5 km/sec

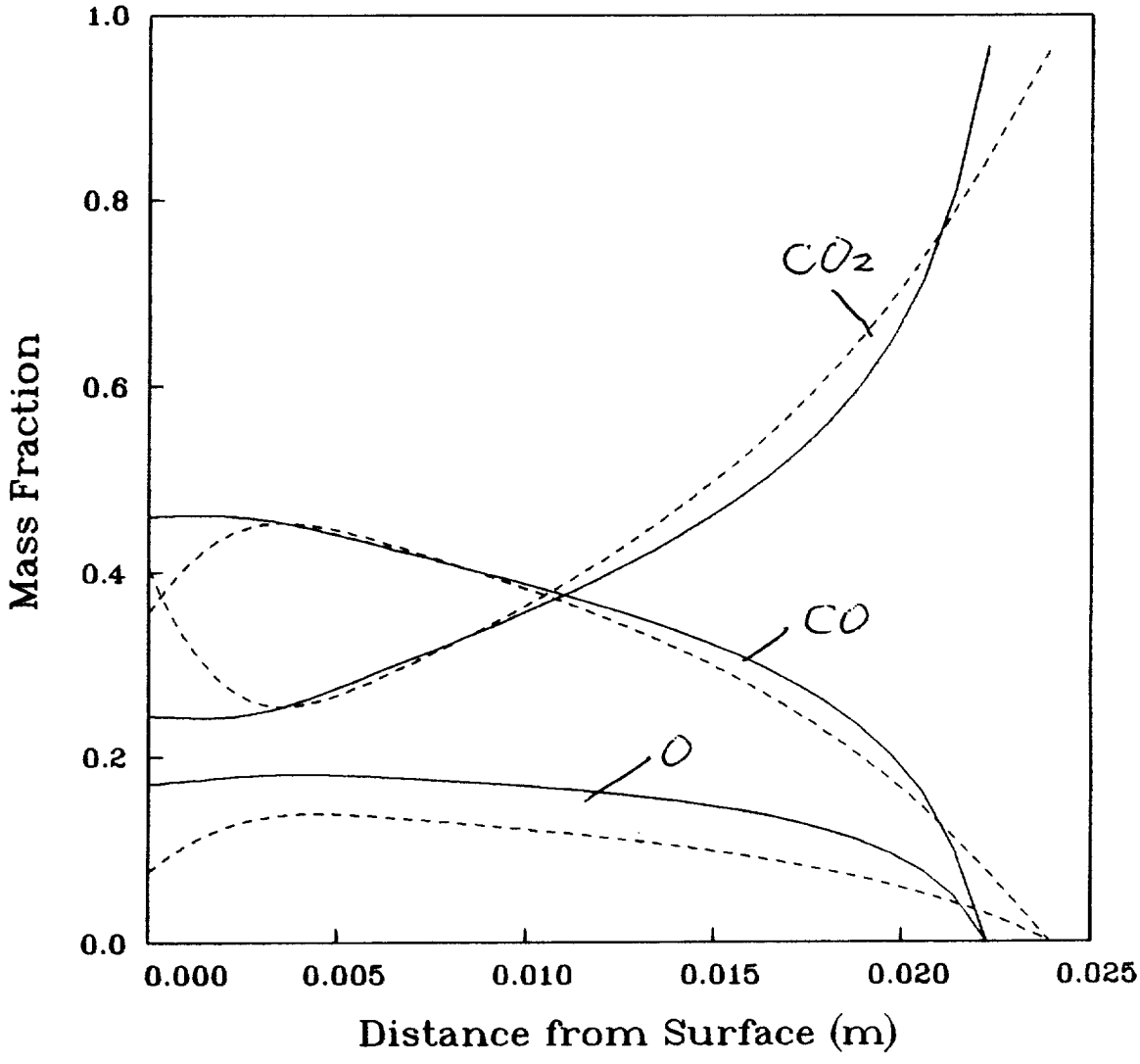

solid line: Park's kinetics
dashed line: McKenzie's kinetics
VSL solution

Fig. 7: Mass Fractions Along Stagnation Streamline
NCW with Tw = 1700 K; Ve = 7 km/sec

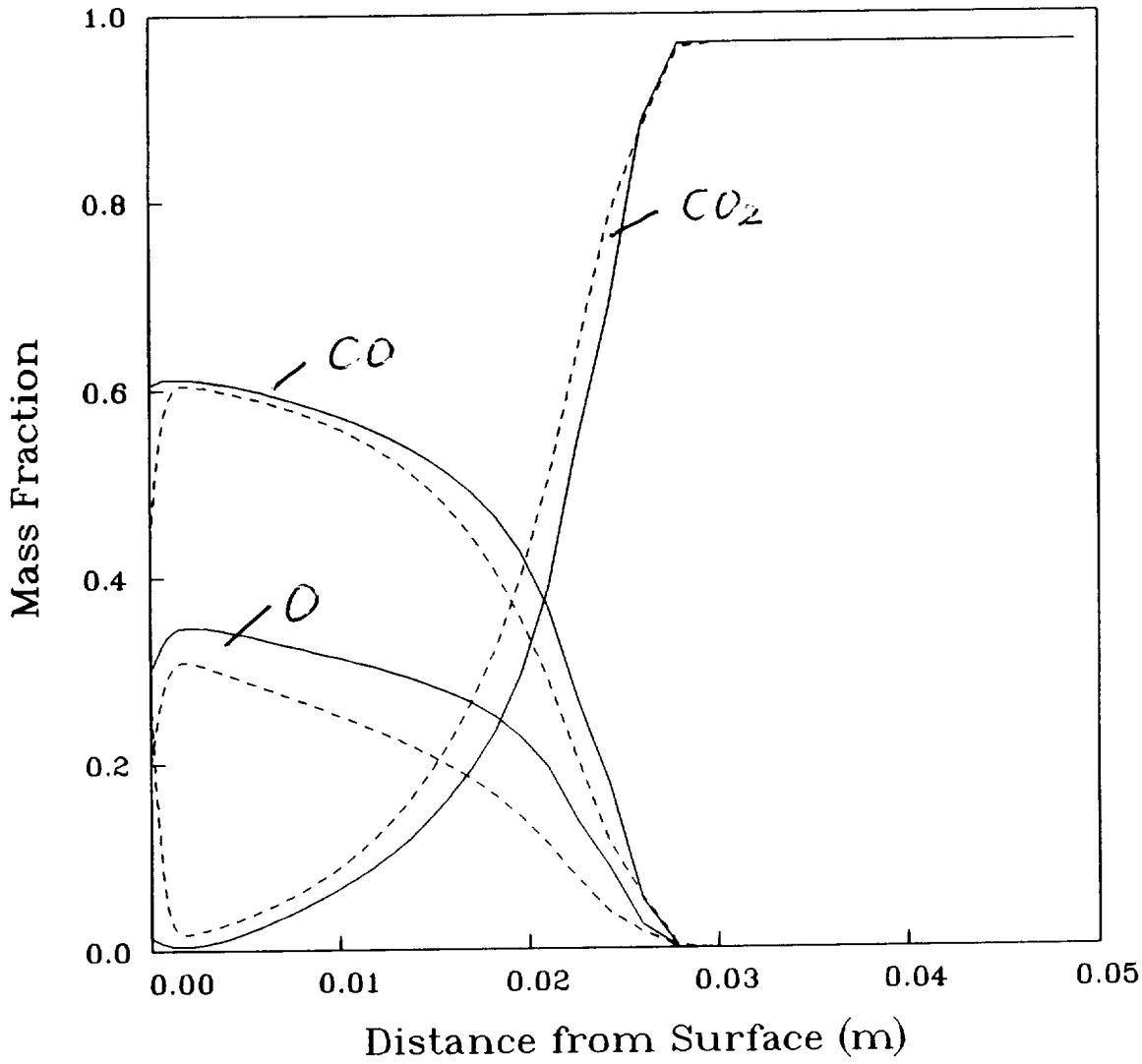

Dashed lines: McKenzie's CO2 recombination rate
Solid lines: Park's CO2 recombination rate
Navier–Stokes solutions

Fig. 8a: Heat Fluxes over Surface
70-degree sphere cone; Ve = 7 km/sec

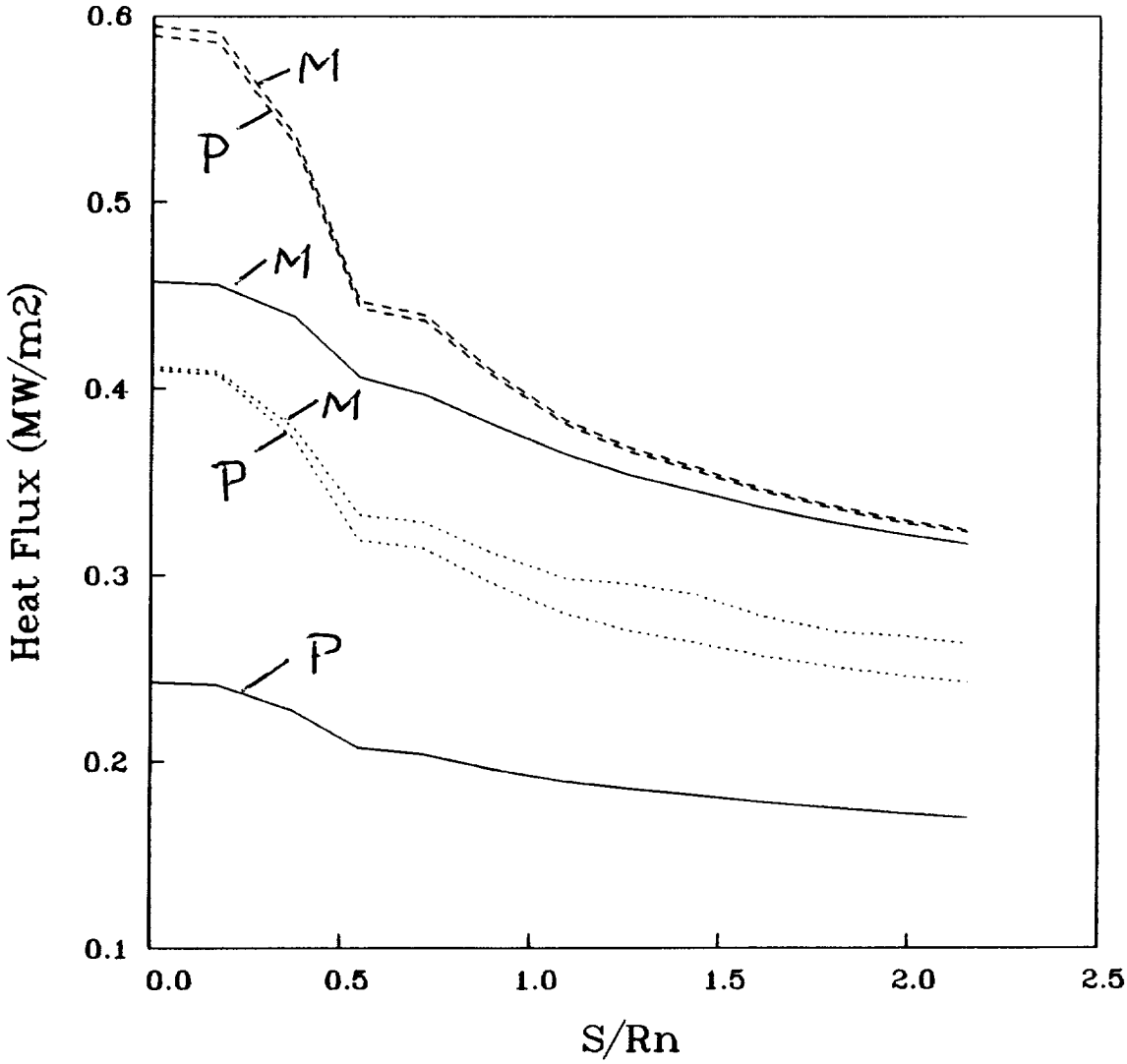

Solid line: Noncatalytic wall
Dashed line: CO + O -> CO2 fully catalytic wall
Dotted line: O + O -> O2 fully catalytic wall
BLIMP (Park's (P) and McKenzie's (M) kinetics)

Fig. 8b: Heat Fluxes over Surface
70-degree sphere cone; EMSI = 0.9; Ve = 7 km/sec

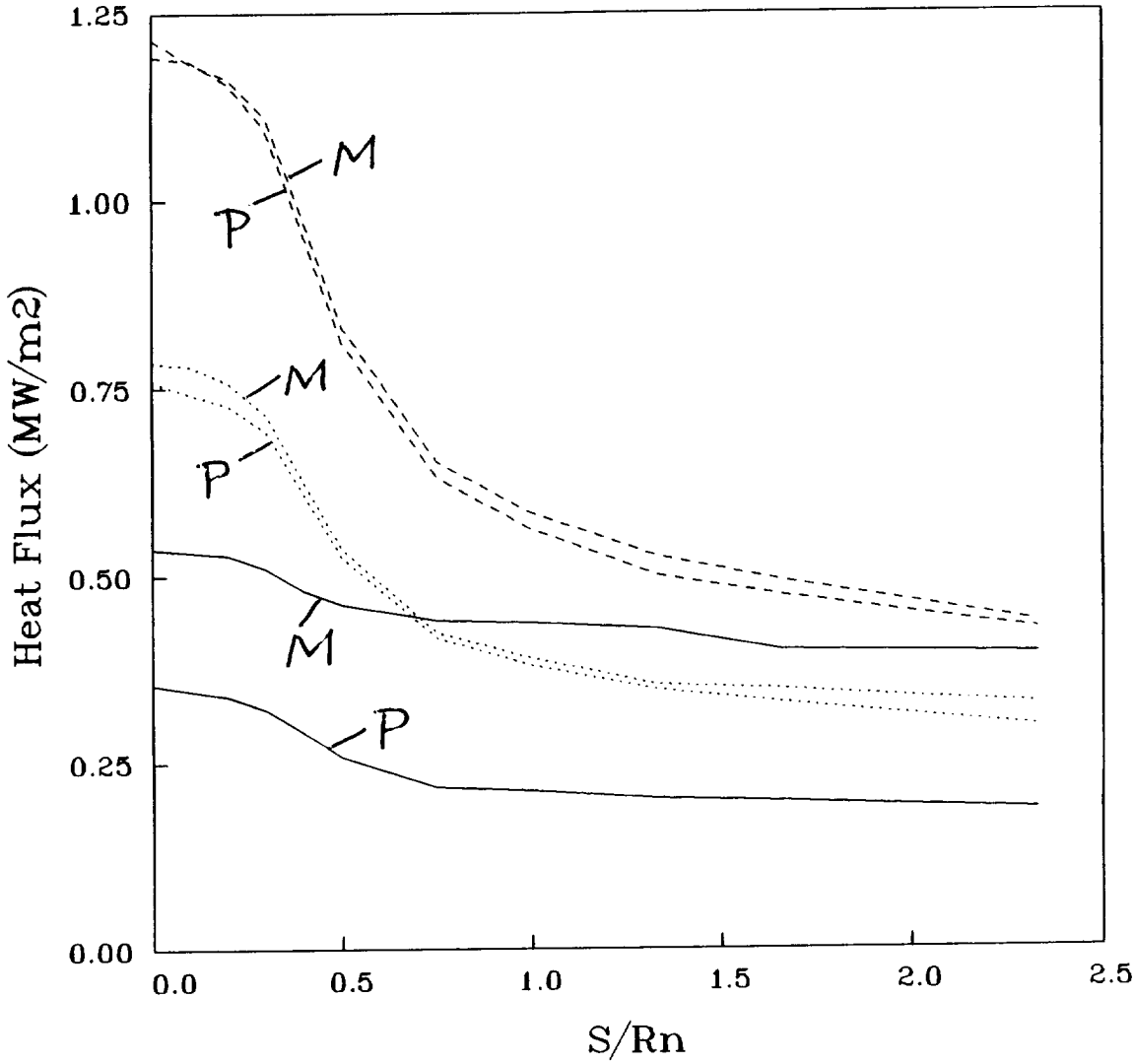

Solid line: Noncatalytic wall
Dashed line: CO + O -> CO2 fully catalytic wall
Dotted line: O + O -> O2 fully catalytic wall
VSL (Park's (P) and McKenzie's (M) kinetics)

Fig. 9a: Surface Heat Fluxes over Surface
MESUR aeroshell; Rn = 0.5 m; Ve = 7 km/sec

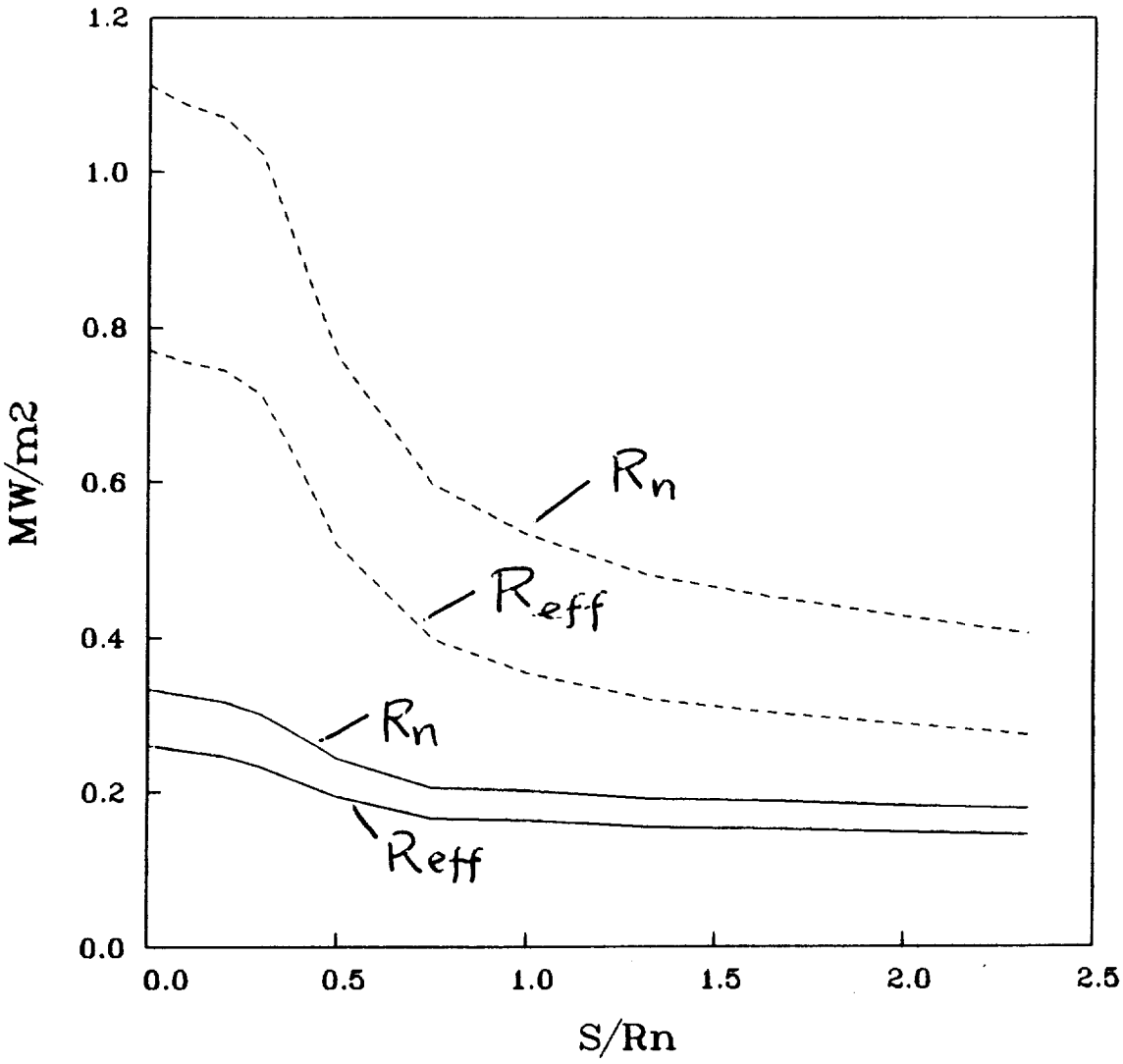

Solid lines: noncatalytic wall
Dashed lines: CO + O –> CO2 fully catalytic wall
VSL solution

Fig. 9b: Surface Heat Fluxes over Surface
MESUR aeroshell; Rn =0.5 m; Ve = 9 km/sec;

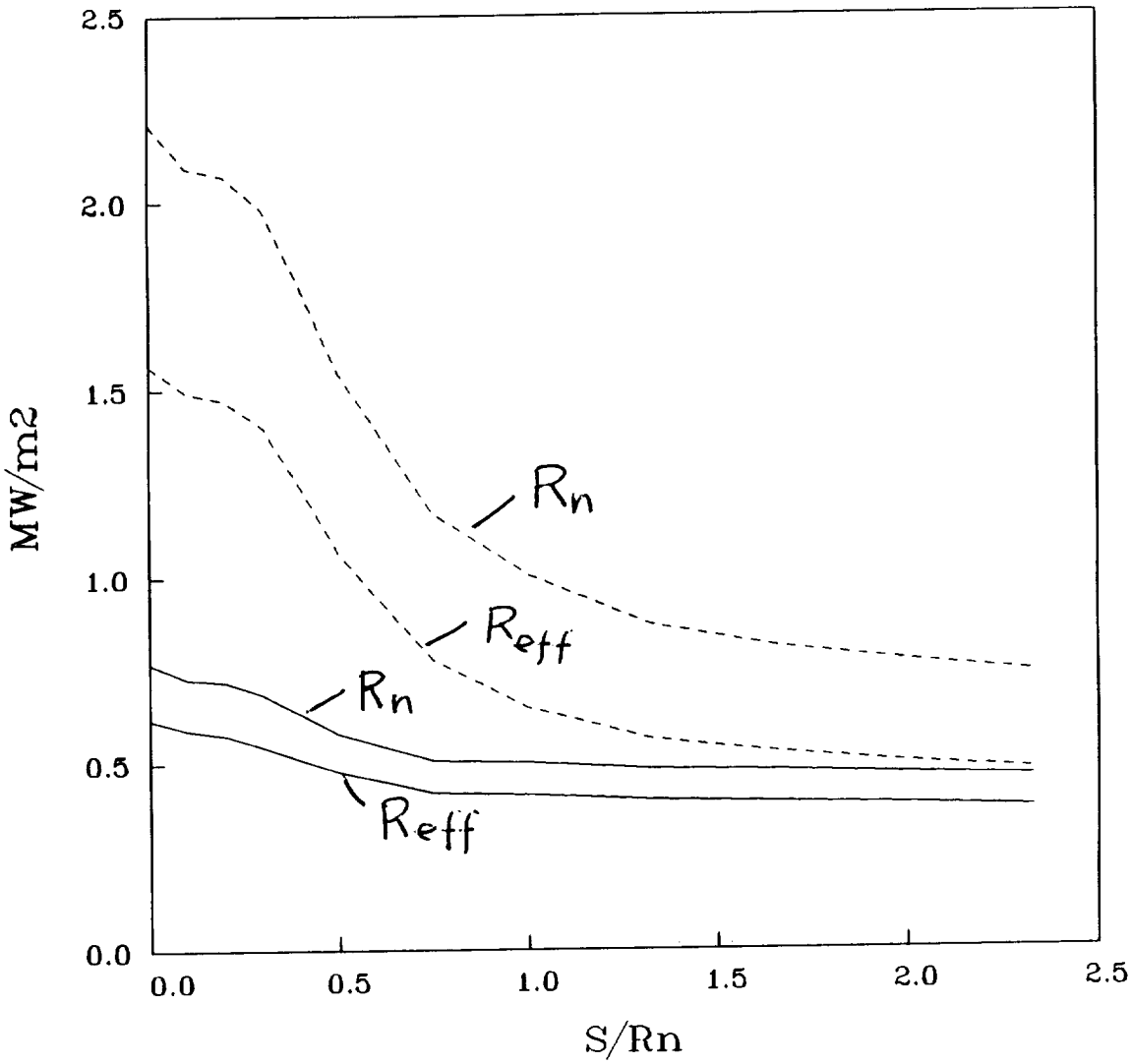

Solid lines: noncatalytic wall
Dashed lines: CO + O -> CO2 fully catalytic wall
VSL solution

REPORT DOCUMENTATION PAGE

Form Approved
OMB No. 0704-0188

1. AGENCY USE ONLY *(Leave blank)*	2. REPORT DATE	3. REPORT TYPE AND DATES COVERED
	September 1992	Contractor Report

4. TITLE AND SUBTITLE

Effect of Non-Equilibrium Flow Chemistry on the Heating Distribution Over the MESUR Forebody During a Martian Entry

5. FUNDING NUMBERS

NAS2-13210

6. AUTHOR(S)

Yih-Kang Chen

7. PERFORMING ORGANIZATION NAME(S) AND ADDRESS(ES)

Sterling Federal Systems, Inc.
1121 San Antonio Road
Palo Alto, CA 94303

8. PERFORMING ORGANIZATION REPORT NUMBER

A-92190

9. SPONSORING/MONITORING AGENCY NAME(S) AND ADDRESS(ES)

National Aeronautics and Space Administration
Washington, DC 20546-0001

10. SPONSORING/MONITORING AGENCY REPORT NUMBER

NASA CR-177601

11. SUPPLEMENTARY NOTES

Point of Contact: Robert A. Carlson, Ames Research Center, MS 233-15, Moffett Field, CA 94035-1000
(415) 604-6036

12a. DISTRIBUTION/AVAILABILITY STATEMENT

Unclassified-Unlimited
Subject Category – 34

12b. DISTRIBUTION CODE

13. ABSTRACT *(Maximum 200 words)*

Effect of flow field properties on the heating distribution over a 140 degree blunt cone was determined for a Martian atmosphere using Euler, Navier–Stokes (NS), viscous shock layer (VSL) and reacting boundary layer (BLIMPK) equations. Effect of gas kinetics on the flow field and surface heating distribution were investigated. Gas models with nine species and nine reactions were implemented into the codes. Effects of surface catalysis on the heating distribution were studied using a surface kinetics model having five reactions.

14. SUBJECT TERMS

Hypersonic flow, Surface catalysis, Non-equilibrium chemistry, Martian entry

15. NUMBER OF PAGES

23

16. PRICE CODE

A02

17. SECURITY CLASSIFICATION OF REPORT	18. SECURITY CLASSIFICATION OF THIS PAGE	19. SECURITY CLASSIFICATION OF ABSTRACT	20. LIMITATION OF ABSTRACT
Unclassified	Unclassified		